**EVOLUTION IN ELECTRICAL AND ELECTRONIC ENGINEERING**
e-ISSN: 2756-8458

**EEEE**

Vol. 5 No. 2 (2024) 359-368
https://publisher.uthm.edu.my/periodicals/index.php/eeee

# Nonlinear Performances of Three-Phase Flux Reversal Motor Employing Modular Rotor for Multi Speed Air Blower

**Muhammad Hazieq Ahnaf Rosnei[1], Mahyuzie Jenal[1]***

[1] *Department of Electrical Engineering, Faculty of Electrical and Electronic Engineering,*
*University Tun Hussein Onn Malaysia, 86400 Parit Raja, Johor, MALAYSIA*

*Corresponding Author: mahyuzie@uthm.edu.my
DOI: https://doi.org/10.30880/eeee.2024.05.02.043

### Article Info

Received: 2 July 2024
Accepted: 30 September 2024
Available online: 30 October 2024

### Keywords

FRM modular rotor, JMAG Designer, three phase, 12 slots, 24 slots, efficiency.

### Abstract

This project tackles the limitations of current air blower systems, which rely on inefficient single-phase power for variable speeds. It focuses objectively on a new design using a three-phase flux reversal motor (FRM) with a modular rotor to achieve efficient multi-speed operation and reduce energy consumption. The project will compare the performance of FRMs with different rotor designs (12 vs 24 slots) to find the most optimal solution. JMAG software was used, with JMAG Geometry Editor for creating motor parts (stators, rotors, etc.) and JMAG Designer for analysis. The Geometry Editor allows for precise sketching with various tools. Once the motor is created, JMAG Designer is used to define materials, conditions, and run simulations. This includes defining the electric circuit (coils) and mesh settings. Finally, the simulation is run to generate results that show motor performance. This study tested the flux linkage of the motor's coils and how it changes with rotation. Then looked at the motor's capabilities under load by increasing the current density. This analysis showed that torque and power increased with current density, while speed decreased. Finally, this study looked at iron and copper losses in the motor at various speeds and found that design 1 offered better overall efficiency. The design (12 coils, 24 coils) was analyzed using JMAG software and showed good performance, especially in efficiency (93%) and power handling. However, the torque is modest (5 Nm). For future work, this study recommends 3D finite element analysis, genetic algorithm optimization, and magnetic field analysis to improve the design further.

## 1. Introduction

In this research explores a new design for high-speed air blowers using a three-phase Flux Reversal Motor (FRM) with a modular rotor. This rotor design is simpler and more reliable compared to traditional ones, making it ideal for high speeds. The project focuses on optimizing the motor's efficiency at various loads by minimizing power loss and achieving smooth torque output across different power levels while the air blower operates. This approach builds upon previous research on optimizing single-phase FRMs and aims to improve efficiency, eliminate torque fluctuations, and prevent negative torque during operation [1]. Overall, the study contributes to the growing interest in FRMs due to their simplicity and suitability for cost-effective, high-speed applications. The objective for this research is to construct a high-speed three-phase flux reversal motor (FRM) featuring modular rotor structure and compare between the three-phase FRM modular rotor 12 slots and 24 slots design performances [2].

## 1.1 Problem Statement

In current air blowers often rely on single-phase power, leading to a significant drawback: inefficiency and subpar performance. This project tackles this challenge head-on by focusing on three key areas. Firstly, it explores a novel motor design - a three-phase Flux Reversal Motor (FRM) with a modular rotor. Understanding the complex non-linear performance of this new design is crucial for optimizing its efficiency. Secondly, the project investigates converting single-phase power to three-phase power. This conversion aims to improve overall energy efficiency, which translates to lower operating costs and a reduced environmental impact. Finally, the project addresses the inherent lower efficiency of single-phase motors by focusing on design optimization to enhance overall efficiency. In a nutshell, this project seeks innovative solutions to revolutionize air blower performance by overcoming the limitations of single-phase power and traditional motor designs. The ultimate goal is to create a more efficient and sustainable air blower system.

## 2. Literature Review

## 2.1 Flux Reversal Motor (FRM)

Flux Reversal Motor (FRM) is a type of doubly salient machine featuring permanent magnets (PMs) located on the stator. In this design, the PM flux linkage within the concentrated coils of the stator phase undergoes a reversal in polarity as the rotor moves. Its uncomplicated structure renders it cost-effective and well-suited for mass production. Notably, the FRM exhibits low self- and mutual inductances, resulting in a reduced electrical time constant and heightened fault tolerance [3]. These advantageous characteristics position the FRM as a potentially significant technology in the realm of automotive generators. However, it's worth mentioning that the FRM does exhibit a noteworthy challenge in the form of PM flux leakage, often attributed to its structural fringing.

## 2.2 Modular Rotor

The modular rotor structure, as opposed to the salient rotor, boasts a reduced iron core size, optimizing the utilization of available rotor iron. This design aims to mitigate the challenges associated with the salient rotor by minimizing the flux route along the rotor. The impetus behind the development of the modular rotor structure stemmed from addressing issues related to flux and losses in the salient rotor configuration. In comparison to alternative rotor designs, the modular rotor not only yields a high average output torque but also requires a notably diminished amount of copper [4]. Fig. 1 demonstrates one of the distinctive features of the modular rotor design is its reliance on mounting all windings and field excitation coils on the stator. This configuration contributes to the stability of the rotor shape in the proposed modular rotor motors [5]. The motivation behind this design choice was informed by the utilization of the finite element method within the JMAG Software, facilitating a comprehensive and meticulous exploration of the rotor's characteristics. The outcome is a modular rotor structure that not only addresses inherent issues associated with the salient rotor but also ensures enhanced efficiency and stability through its unique design and optimized use of materials [6].

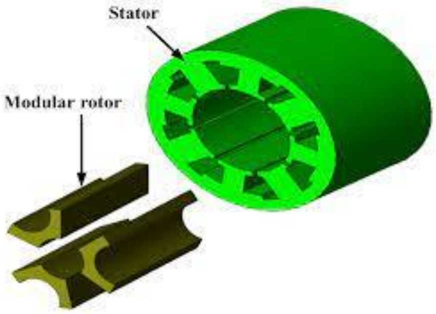

**Fig. 1** *FEFSM with modular rotor design [5]*

## 2.3 Three Phase

In the realm of operating with three phases of alternating current (AC), the preeminent choice for a motor is the three-phase electric motor, given its widespread application and the notable advantage of not necessitating an external starting device. Unlike their single-phase counterparts, these motors are inherently self-starting AC motors. The construction of a winding circuit for a three-phase motor is intricately tied to the number of slots in the motor, with the windings designed to generate a single rotating magnetic field during changes in the AC supply source [7]. The operational principle of a three-phase motor emphasizes a crucial aspect ensuring that the rotor's speed does not approach the synchronous speed of the stator. Fig. 2 illustrates this principle, as the precaution is essential because if the two speeds were to coincide, no electromotive force (emf) would be induced in the rotor, leading to a lack of current flow. Without the flow of current, the motor would be unable to generate the necessary torque for its functioning. The concept of "slip" becomes pivotal in this context, representing the differential in speed that exists between the rotor and the stator [8]. It's worth noting that three-phase electric motors find extensive use in both residential and industrial settings, particularly in situations where precise speed control is not a prerequisite. This underscores their practicality and efficiency in various applications where a constant speed suffices for optimal performance.

**Fig. 2** *Example of the 3-phase motors application air compressor and laundry pressing machine [9]*

## 3. Methodology

For the methodology, this section outlines the methodology employed to accomplish the first and second objectives of the study. The primary goals are to propose a Flux Reversal Motor (FRM) with a modular-shaped rotor structure and analyze the motor's performances and efficiency under various operational loads. When introducing a new structure, it is imperative to conduct tests to ascertain the smooth operation of the motor. The process commences with the systematic sketching of each motor part in the geometry editor, followed by further development in the designer. In the designer, materials and conditions are specified for subsequent analysis and simulation. This step-by-step approach ensures a comprehensive exploration of the motor's design and performance characteristics.

### 3.1 Parameter and Materials

The table below compares the design parameters of a stator and rotor, likely for a high-speed, three-phase Flux Reversal Motor (FRM) intended for an air blower application. Separated into Table 1 and Table 2, the table details specifications like the number of poles and slots, radius measurements, and material types. This information provides a clear picture of the design choices made for the stator and rotor in this high-speed FRM air blower system.

**Table 1** *Parameter of the proposed rotor and stator*

| Parameter | Value |
|---|---:|
| Stator poles | 6 / 12 |
| Stator slots | 12 / 24 |
| Rotor poles | 10 |
| Outer radius of stator, (mm) | 50 |
| Inner radius of stator, (mm) | 33.5 |
| Outer radius of rotor, (mm) | 28 |
| Inner radius of rotor, (mm) | 10 |
| Airgap length, (mm) | 0.5 |
| Motor stack length, (mm) | 70 |
| No of turn per coil | 101 / 51 |

**Table 2** *Materials and Condition*

| Parts | Materials | Conditions |
|---|---|---|
| Rotor | Nippon Steel 35H210 | Motion: Rotation<br>Torque: Nodal Force |
| Stator | Nippon Steel 35H210 | - |
| Armature Coils | Conductor Copper | FEM Coil |

## 3.2 System Flowchart of Overall Project

This section outlines the methodology employed to accomplish the first and second objectives of the study. The primary goals are to propose a Flux Reversal Motor (FRM) with a modular-shaped rotor structure and analyze the motor's performances and efficiency under various operational loads. When introducing a new structure, it is imperative to conduct tests to ascertain the smooth operation of the motor. As depicted in Fig. 3, starting with the systematic sketching of each motor part in the geometry editor, followed by further development in the designer. In the designer, materials and conditions are specified for subsequent analysis and simulation. This step-by-step approach ensures a comprehensive exploration of the motor's design and performance characteristics.

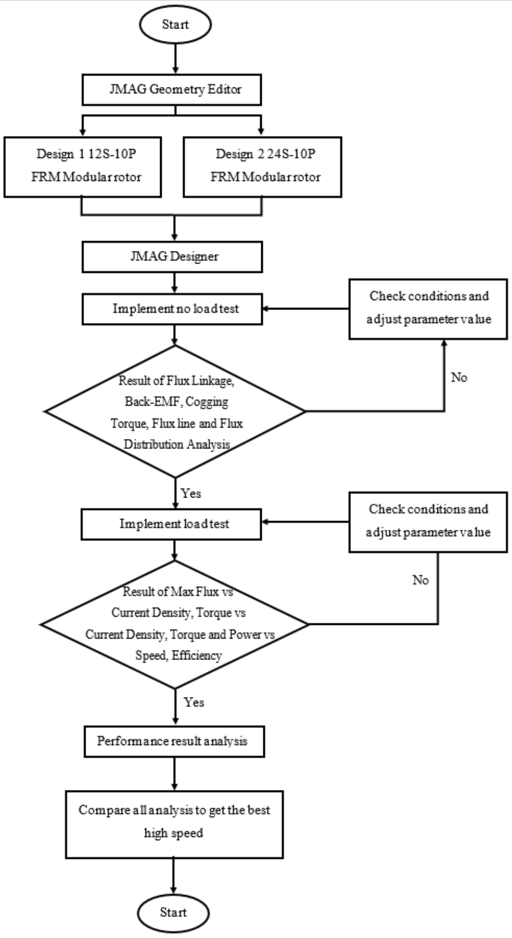

**Fig. 3** *Overall implementation of the study*

## 3.3 Formula Use in Simulation

This section likely presents formulas used in JMAG Designer software for defining coil properties and simulation settings. Equations (1), (2), and (3) might be related to calculating the number of turns needed for a coil in motor design, influencing factors like magnetic field strength. Equations (4) and (5) seem to focus on simulation control. Equation (4) might help determine the total simulation time, while equation (5) might be used to calculate frequencies relevant to analyzing motor behavior under various operating conditions. While JMAG Designer offers functionalities to handle these calculations based on user input, understanding the underlying formulas (e.g., effective area, number of turns per layer, coil area, end time, and frequency) can provide valuable insights into your motor design and simulation setup.

$$N_a = \frac{A_{eff}}{A_{coil}} \tag{1}$$

$$A_{eff} = A(0.5) \tag{2}$$

$$A_{coil} = \pi(0.5^2) \tag{3}$$

$$t_e = \frac{1}{f_e} \tag{4}$$

$$f_e = \frac{n.N_r}{60} \tag{5}$$

## 4. Result and Discussion

In this analysis for Fig. 4, the no load test sets the armature current density to zero and assumes a constant permanent magnet flux linkage. This allows for studying the maximum achievable magnetic flux and its distribution within the motor. Additionally, back EMF and cogging torque are examined at specific angles. While in load test analysis evaluates motor performance under various load conditions. It simulates increasing the armature current density from zero to a certain value (e.g., 30 Arms/mm2). By analyzing factors like torque, power, speed, losses, and efficiency, the load state of the motor is determined. The recommended design's peak and RMS armature currents are provided in tables for further load analysis within the software.

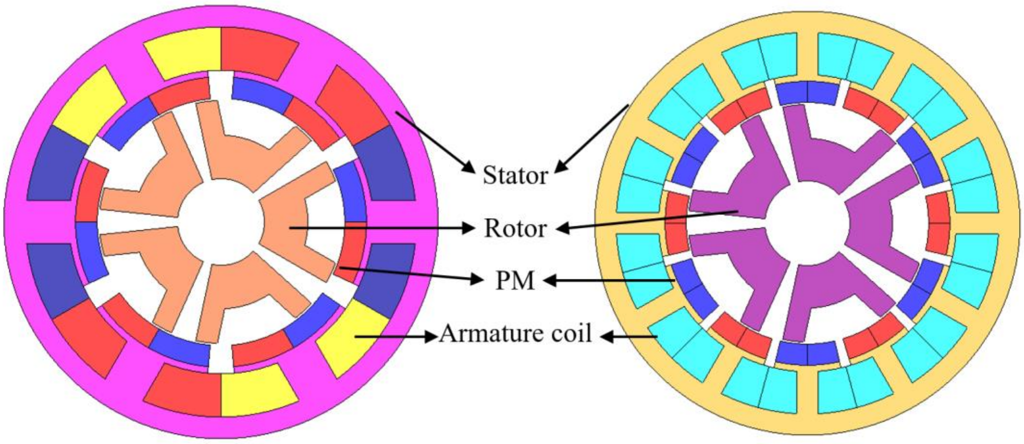

**Fig. 4** *Proposed design of 12S-10P and 24S-10P FRM*

## 4.1 Flux Linkage Analysis

A coil test procedure was used to analyze the flux linkage in order to identify the distinct flux linkage patterns produced by each armature coil and assess the properties of these linkages. The armature coils have a set polarity and wind in a clockwise manner. The permanent magnets (PMs), on the other hand, alternate between each other and are oriented in opposite orientations. Tests are conducted on the coil flux linkage when the motor is operating at 1200 rpm. Fig. 5 and Fig. 6, correspondingly, graphically represent the coil test results for design variants 1 and 2.

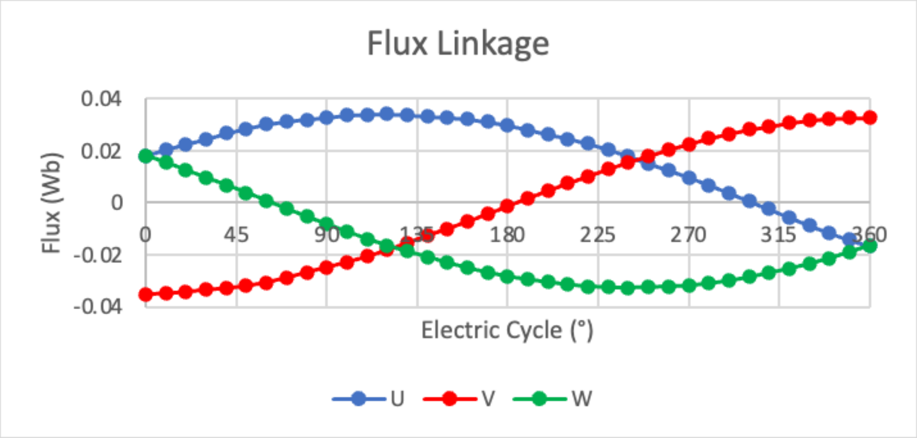

**Fig. 5** *Graph of coil flux linkage proposed design 1*

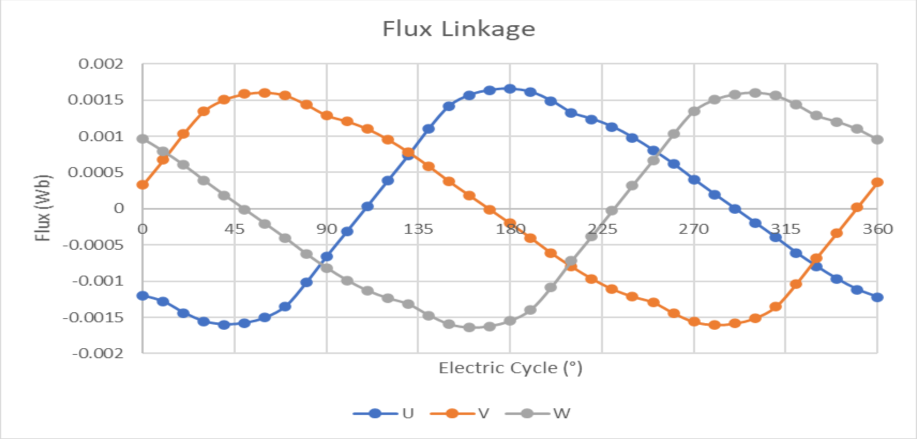

**Fig. 6** *Graph of coil flux linkage proposed design 2*

## 4.2 Cogging Torque

In essence, cogging torque is the outcome of the permanent magnet (PM) of the rotor interacting with the stator slots. This process may compromise the overall integrity of the motor structure by causing undesirable consequences as vibration, resonances, noise, and speed ripples. Fig. 7 and Fig. 8 provide a visual representation of the cogging torque for the proposed designs 1 and 2 Flux Reversal Motors (FRM). The figure shows that, for suggested design 1, the cogging torque for the no load test has a peak-to-peak value of 1.187 Nm at 330 degrees at the highest and -1.623 Nm at 70 degrees at the lowest. On the other hand, the maximum and lowest values for the suggested design 2 vary from 0.264 Nm to -0.242V. It is important to remember that torque levels higher than 10% of the average torque may cause excessive vibration, which highlights how critical cogging torque management is to achieving the best possible motor performance.

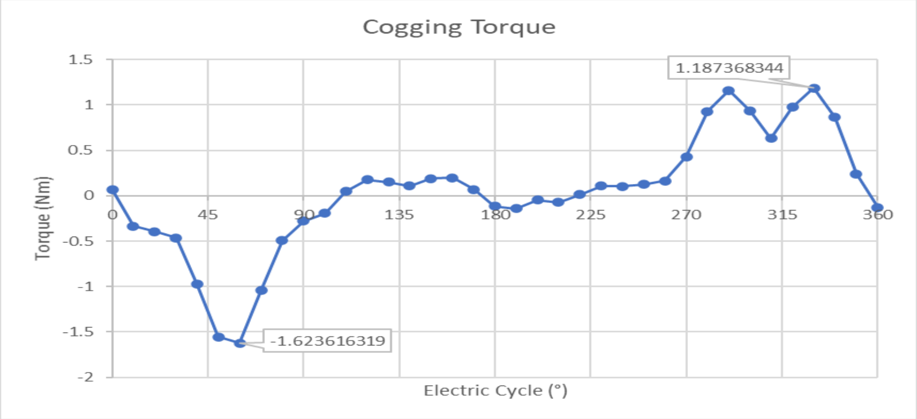

**Fig. 7** *Graph of cogging torque of proposed design 1*

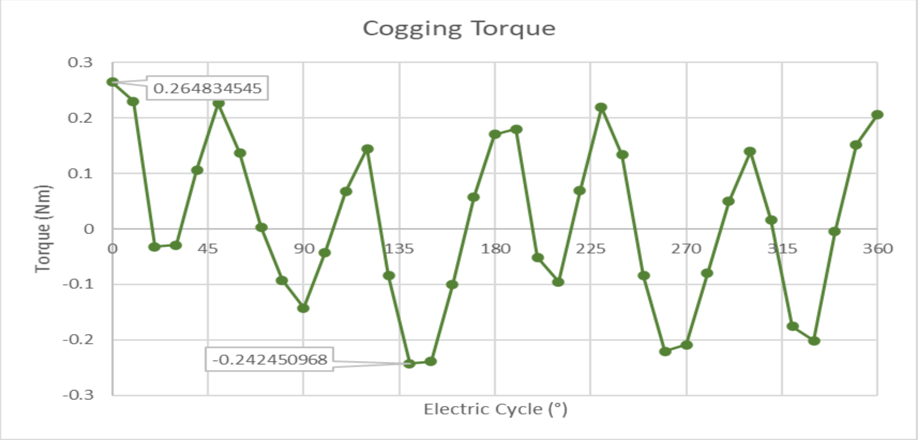

**Fig. 8** *Graph of cogging torque of proposed design 2*

## 4.3 Load Analysis

If it hasn't previously been assessed, the motor's performance under load conditions may be examined. The load test condition may be performed by changing the armature current density from 0 Arms/mm2 to 30 Arms/mm2. Numerous variables, including torque performance, power, speed, iron and copper losses, and efficiency, are taken into account to establish the load condition of the motor. Table 3 and Table 4, which may be seen below, show the peak and rms armature current values associated with the proposed design. The estimated current density will be used to do a load condition analysis via the process of entering the values into the circuit.

**Table 3** *Armature current density proposed design 1*

| Armature Current Density, ($J_a$) | $I_a$ peak | $I_a$ *rms* |
|---|---|---|
| 5 | 3.9433 | 5.5766 |
| 10 | 7.8866 | 11.1533 |
| 15 | 11.8299 | 16.7300 |
| 20 | 15.7732 | 22.3066 |
| 25 | 19.7165 | 27.8833 |
| 30 | 23.6599 | 33.4601 |

**Table 4** *Armature current density proposed design 2*

| Armature Current Density, ($J_a$) | $I_a$ peak | $I_a$ *rms* |
|---|---|---|
| 5 | 3.9068 | 5.5250 |
| 10 | 7.8137 | 11.0502 |
| 15 | 11.7205 | 16.5753 |
| 20 | 15.6275 | 22.1006 |
| 25 | 19.5343 | 27.6256 |
| 30 | 23.4411 | 33.1507 |

## 4.4 Maximum Flux vs Armature Current Density

The capability of motor can be observed by the value of torque, power and speed characteristic. The power of high-speed three-phase modular rotor FRM has been observed with respect to armature current density 0 $Arms/mm2$ to 30 $Arms/mm2$. The power increase as the heat is generated. Fig. 9 and Fig. 10 show the maximum flux vs armature current density increase proportional for both graphs. For the FRM modular rotor proposed design 1, the total U-phase flux interaction at different Ja is about 0.179Wb, whereas for proposed design 2, it is 0.068Wb, as seen in Fig. 8 and Fig. 9.

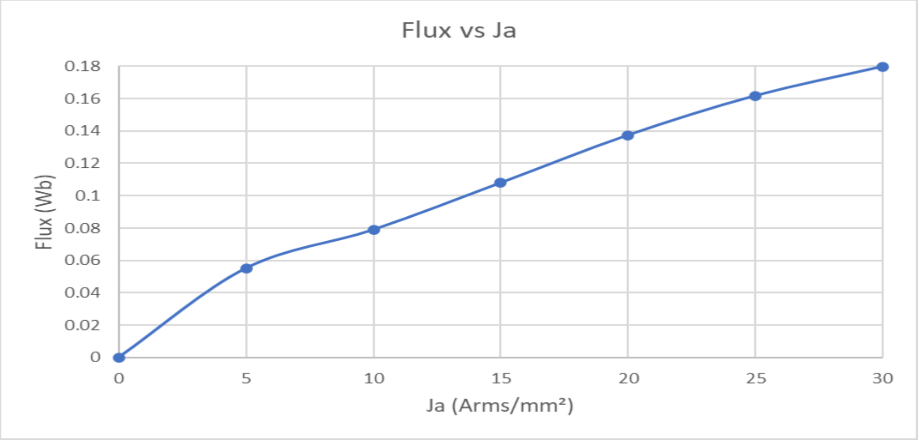

**Fig. 9** *Flux vs Armature current density characteristic design 1*

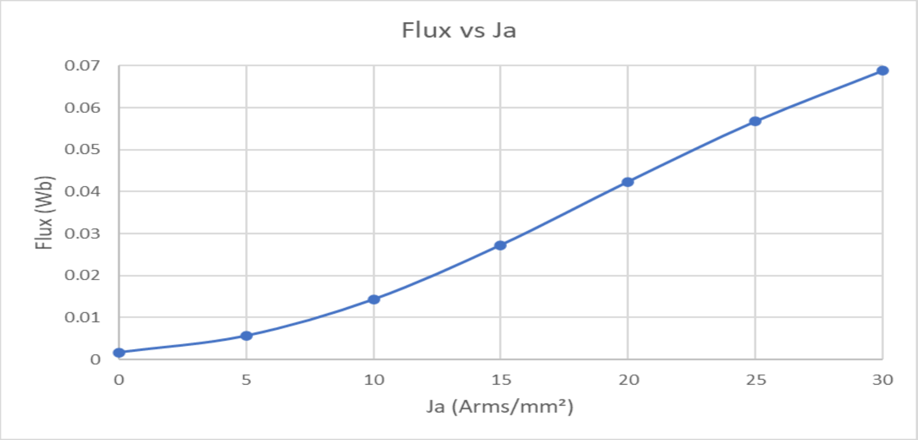

**Fig. 10** *Flux vs Armature current density characteristic design 2*

## 4.5 Power Losses and Efficiency

Iron loss (Pi) and copper loss (Pc) are the two forms of losses that may occur in motors. Losses are specified by 19 and 17 points from the value of beneath the graph that shows the relationship between torque and speed. A further investigation of the power losses and efficiency of the suggested design 1 was carried out. At a variety of speed ranges, Fig. 11 and Fig. 12 illustrates 19 and 17 points that represent high, moderate, and low levels of torque throughout the board. On the basis of the findings, point 6 was shown to have the lowest iron losses at the lowest speed, which was 100.00 revolutions per minute. On the other hand, point 2 had the greatest value of iron losses, which was 29.24 kW, at the maximum speed, which was 1446.20 revolutions per minute. In spite of this, the motor in consideration has an efficiency of 59.24% on average.

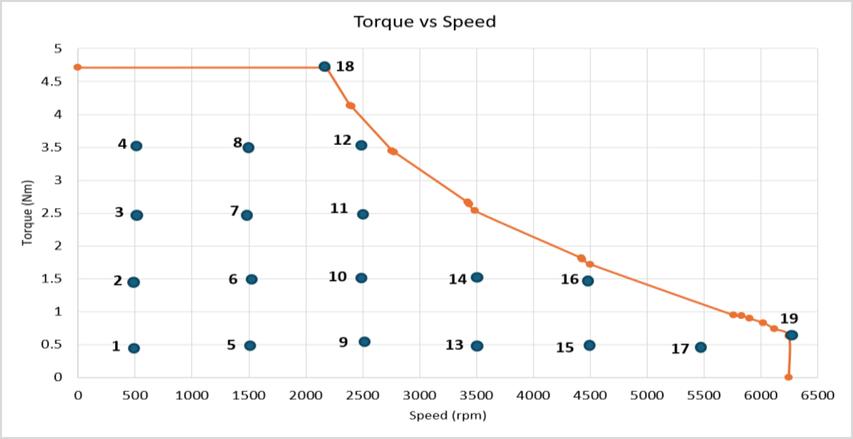

**Fig. 11** *Points under the graph of torque vs speed design 1*

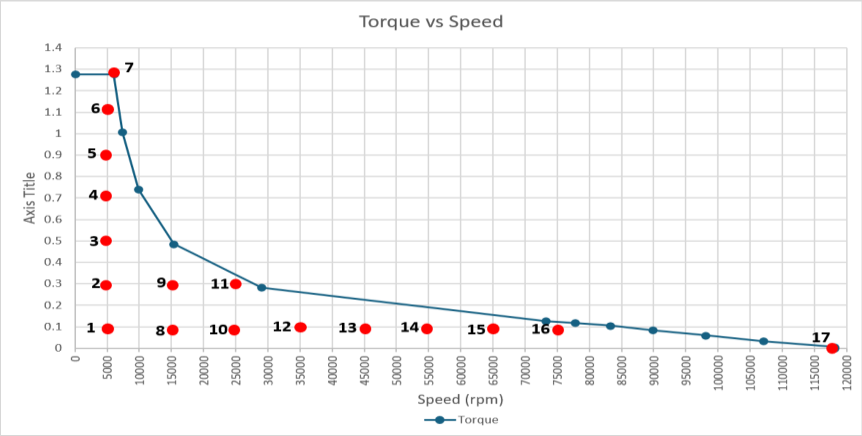

**Fig. 12** *Points under the graph of torque vs speed design 2*

## 4.6 Comparison between all designs

The performance and capability of the electric motor of a high-speed three-phase FRM modular rotor with two proposed designs were compared to identify the optimal design of the motor. Table 5 provides a detailed comparison based on several key parameters. The Maximum Speed (rpm) refers to the highest rotational speed the motor can achieve. Efficiency (η %) indicates the percentage of input power that is converted into useful output power. Power Output (kW) measures the amount of useful power the motor produces, while Power Loss (kW) represents the power lost due to inefficiencies. Total Power (kW) denotes the total power consumed by the motor. The Maximum U-Flux (Wb) is the peak magnetic flux in the motor, and Maximum Torque (Nm) indicates the highest torque the motor can generate. Lastly, Maximum Current (A) is the highest current the motor draws. By examining these parameters, we can evaluate and compare the performance and efficiency of different motors.

**Table 5** *Comparison data of both proposed design*

| Comparison | Proposed Design 1<br>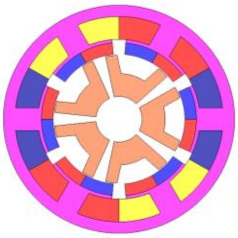 | Proposed Design 2<br>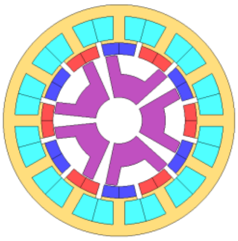 |
|---|---|---|
| Highest Speed, rpm | 6241.80 | 118077.08 |
| Efficiency, η (%) | 93.13 | 0.73 |
| Power Output, W | 3902.81 | 637.56 |
| Power Loss, W | 288.10 | 86323.44 |
| Total Power, W | 4190.90 | 86961.00 |
| Output U-Flux, Wb | 0.18 | 0.069 |
| Output Torque, Nm | 5 | 0.1 |
| Input Current, A | 5.57 | 33.15 |

## 5. Conclusion

In this study explored a new design for high-speed air blowers: a "12S-10P and 24S-10P FRM with modular rotor" designed using JMAG 18.1 software. The research involved analyzing and optimizing this design compared to a preliminary version. A crucial aspect was understanding the motor's three-phase operation through detailed analysis of the coil configuration (12-coil, 24-coil, UVW). Additional analyses focused on cogging torque, magnetic flux distribution, and no-load performance. The project identified "Proposed Design 1" as particularly promising. It shines in several areas: exceptional high speed (6241.80 rpm), impressive efficiency (93.13% conversion of input power to usable output), and noteworthy power handling capability (3902.81 kW). While there is some power loss (288.10 kW), it's minimal compared to the overall power, further highlighting the design's efficiency. Additionally, the U-Flux and maximum current stay within acceptable limits, suggesting good magnetic load management and minimal electrical losses. However, a key limitation of Proposed Design 1 is its modest maximum torque (5 Nm). This could be a disadvantage for applications requiring high torque.

## Acknowledgement

The authors would also like to thank the Faculty of Electrical and Electronic Engineering, Universiti Tun Hussein Onn Malaysia for its support.

## Conflict of Interest

Authors declare that there is no conflict of interests regarding the publication of the paper.

## Author Contribution

The author attests to having sole responsibility for the following: planning and designing the study, data collection, analysis and interpretation of the outcomes, and paper writing.

## References

[1] T. H. Kim and J. Lee, “A Study of the Design for the Flux Reversal Machine,” IEEE transactions on magnetics, vol. 40, no. 4, pp. 2053–2055, Jul. 2004, doi: https://doi.org/10.1109/tmag.2004.832488.

[2] D. J. Powell, G. W. Jewell, S. D. Calverley, and D. Howe, “Iron loss in a modular rotor switched reluctance machine for the ‘more-electric’ aero-engine,” INTERMAG Asia 2005. Digests of the IEEE International Magnetics Conference, 2005., Jan. 2005, doi: https://doi.org/10.1109/intmag.2005.1463470.

[3] R. Deodhar, Sven Ingmar Andersson, Ion Boldea, and T. J. E. Miller, “The flux-reversal machine: a new brushless doubly-salient permanent-magnet machine,” IEEE Transactions on Industry Applications, vol. 33, no. 4, pp. 925–934, Jan. 1997, doi: https://doi.org/10.1109/28.605734.

[4] Ishikawa, Takeo & Xie, Peijie & Kurita, Nobuyuki, “Topology Optimization of Rotor Structure in Permanent Magnet Synchronous Motors Considering Ease of Manufacturing,” 2015 IEEJ Journal of Industry Applications. 4. 469-475. 10.1541/ieejjia.4.469.

[5] W. Ullah, F. Khan and M. Umair, "Optimal rotor poles and structure for design of consequent pole permanent magnet flux switching machine," in Chinese Journal of Electrical Engineering, vol. 7, no. 1, pp. 118-127, March 2021, doi: 10.23919/CJEE.2021.000011.

[6] Evgenij Koptjaev and A. J. Marques, “A Single-Phase Brushless 4 Slots-4 Poles Flux Switching Generator with Modular Rotor,” Sep. 2023, doi: https://doi.org/10.1109/uralcon59258.2023.10291147.

[7] Yuting Gao, Ronghai Qu, Dawei Li and Jian Li, "Torque performance analysis of three-phase flux reversal machines for electric vehicle propulsion," 2016 IEEE Transportation Electrification Conference and Expo, Asia-Pacific (ITEC Asia-Pacific), Busan, 2016, pp. 296-301, doi: 10.1109/ITEC-AP.2016.7512966.

[8] Y. Gao, R. Qu, D. Li and J. Li, "Torque Performance Analysis of Three-Phase Flux Reversal Machines," in IEEE Transactions on Industry Applications, vol. 53, no. 3, pp. 2110-2119, May-June 2017, doi: 10.1109/TIA.2017.2677356.

[9] Y. Gao, R. Qu, J. Li, D. Li and L. Wu, "Power factor of three-phase flux reversal machines," 2015 IEEE International Magnetics Conference (INTERMAG), Beijing, China, 2015, pp. 1-1, doi: 10.1109/INTMAG.2015.7156551.